JOURNAL OF BACTERIOLOGY, Dec. 2011, p. 6539–6551 Vol. 193, No. 23
0021-9193/11/$12.00 doi:10.1128/JB.05924-11
Copyright © 2011, American Society for Microbiology. All Rights Reserved.

Peroxide Stimulon and Role of PerR in Group A *Streptococcus*▽†

Renata Grifantini,[1]‡§ Chadia Toukoki,[2,3]‡ Annalisa Colaprico,[1] and Ioannis Gryllos[2,3]*

Novartis Vaccines and Diagnostics, Via Fiorentina 1, 53100 Siena, Italy,[1] and Division of Infectious Diseases, Children's Hospital Boston[2] and Harvard Medical School,[3] Boston, Massachusetts 02115

Received 3 August 2011/Accepted 18 September 2011

We have characterized group A *Streptococcus* (GAS) genome-wide responses to hydrogen peroxide and assessed the role of the peroxide response regulator (PerR) in GAS under oxidative stress. Comparison of transcriptome changes elicited by peroxide in wild-type bacteria with those in a *perR* deletion mutant showed that 76 out of 237 peroxide-regulated genes are PerR dependent. Unlike the PerR-mediated upregulation of peroxidases and other peroxide stress defense mechanisms previously reported in Gram-positive species, PerR-dependent genes in GAS were almost exclusively downregulated and encoded proteins involved in purine and deoxyribonucleotide biosynthesis, heme uptake, and amino acid/peptide transport, but they also included a strongly activated putative transcriptional regulator (*SPy1198*). Of the 161 PerR-independent loci, repressed genes (86 of 161) encoded proteins with functions similar to those coordinated by PerR, in contrast to upregulated loci that encoded proteins that function in DNA damage repair, cofactor metabolism, reactive oxygen species detoxification, pilus biosynthesis, and hypothetical proteins. Complementation of the *perR* deletion mutant with wild-type PerR restored PerR-dependent regulation, whereas complementation with either one of two PerR variants carrying single mutations in two predicted metal-binding sites did not rescue the mutant phenotype. Metal content analyses of the recombinant wild type and respective PerR mutants, in addition to regulation studies in metal-supplemented and iron-depleted media, showed binding of zinc and iron by PerR and an iron requirement for optimal responses to peroxide. Our findings reveal a novel physiological contribution of PerR in coordinating DNA and protein metabolic functions in peroxide and identify GAS adaptive responses that may serve to enhance oxidative stress resistance and virulence in the host.

Group A *Streptococcus* (GAS) (*Streptococcus pyogenes*) infections vary from superficial infection of the pharynx (strep throat) to serious skin and soft tissue infections that can lead to lethal invasive disease despite antibiotic treatment (10, 51). Resistance mechanisms of GAS to oxidative damage and killing by reactive oxygen species (ROS), which are generated from atmospheric oxygen or are produced by the phagocyte oxidative burst, have been partially characterized. Peroxidases, such as alkyl hydroperoxidase/alkyl hydroperoxide reductase (*ahpCF*) and glutathione peroxidase (*gpoA*), neutralize organic and inorganic peroxides and contribute to GAS aerotolerance and ROS detoxification *in vitro* (5, 33). The significance of these enzymes to bacterial fitness *in vivo* remains unclear, as *ahpC* and *gpoA* mutants show moderate reduction of virulence following subcutaneous and intraperitoneal infection in mice, respectively (5, 6). Resistance to superoxide (O_2^-) toxicity is mediated by superoxide dismutase (*sodA*) that converts O_2^- to H_2O_2, which is detoxified in turn by peroxidases (17). A critical role for SodA in GAS aerobic growth has been proposed (18). The iron/DNA-binding protein Dpr/MrgA (Dps-like peroxide resistance protein) is also thought to contribute to resistance against oxidative DNA damage by chelating free intracellular iron, thus preventing its reaction with peroxide (Fenton reaction) and leading to generation of highly reactive hydroxyl radicals (5, 65).

Defenses of GAS against ROS are coordinated, in part, by the peroxide stress response transcriptional regulator PerR. Earlier studies recorded significant virulence attenuation of *perR* mutants following subcutaneous or intraperitoneal inoculation in mice (5, 56), while recent investigations showed a role for PerR-controlled gene expression in GAS resistance to ROS-mediated killing by phagocytes and a critical contribution to pharyngeal colonization (21). To date, the extent of the PerR regulon and its contribution to GAS physiology under oxidative stress remain incompletely defined. In *Bacillus* and *Staphylococcus*, PerR activates expression of peroxidases and Dpr/MrgA under peroxide stress and coordinates iron homeostasis in order to minimize ROS formation via the Fenton reaction (12, 25, 27). Transcriptome comparisons between wild-type M-type 5 GAS and an isogenic *perR* mutant grown in the absence of stress indicated PerR-dependent repression (3-fold or higher) of six genes. These genes included *pmtA* encoding a putative metal efflux protein and additional loci encoding proteins with predicted function in zinc and/or manganese homeostasis and transport. Whereas *pmtA* is under direct PerR control, repression of the remaining five genes is thought to be an indirect effect mediated by a second transcriptional regulator, AdcR (7). Similar transcriptome comparisons between wild-type and *perR* mutant bacteria in M-type 3 GAS confirmed PerR-dependent repression of *pmtA* and AdcR-regulated loci but also suggested moderate repression of *ahpCF* and other loci and upregulation of several sugar transport genes (21). Promoter sequences of *pmtA* and *ahpCF* carry

* Corresponding author. Mailing address: Division of Infectious Diseases, Children's Hospital Boston, 300 Longwood Avenue, Boston, MA 02115. Phone: (617) 919-2908. Fax: (617) 730-0254. E-mail: ioannis.gryllos@childrens.harvard.edu.

† Supplemental material for this article may be found at http://jb.asm.org/.

‡ R.G. and C.T. contributed equally to this work.

§ Present address: Externautics Spa, Via Fiorentina 1, 53100 Siena, Italy.

▽ Published ahead of print on 23 September 2011.

fully conserved Per boxes and have been shown to bind recombinant PerR *in vitro*; however, PerR control of *ahpCF in vivo* remains unclear, as this locus is marginally derepressed in two *perR* mutant strains (5, 21). These analyses identified GAS loci coordinated by PerR at baseline but did not examine the contribution of this regulator to GAS responses in the presence of a physiological oxidative stimulus.

We now define global responses of wild-type and *perR* mutant GAS to H_2O_2 and assess the role of PerR as a ROS sensor in this pathogen. Further genetic and biochemical analyses provide insight into the molecular mechanism of PerR function in streptococci. These studies characterize for the first time the peroxide stimulon of GAS and identify PerR-dependent and -independent defense mechanisms elicited by oxidative stress.

MATERIALS AND METHODS

Bacterial strains and growth conditions. GAS strain 003Sm is a streptomycin-resistant variant of M-type 3 strain DLS003 isolated from a patient with necrotizing fasciitis (21), whereas strain 854 is an M-type 1 strain isolated from a retroperitoneal abscess (23). Mutant strain 003Sm*perR*Δ (or *perR*Δ) lacking over 80% of *perR* has been described previously (21). GAS was grown at 37°C in Todd-Hewitt broth (Difco Laboratories) supplemented with 0.5% yeast extract (THY) or on THY agar or Trypticase soy agar, both supplemented with 5% defibrinated sheep blood. For cloning, *Escherichia coli* DH5α or XL1-Blue was grown in Luria-Bertani (LB) broth or on LB agar. When appropriate, the following antibiotics were added at the concentrations indicated: ampicillin, 100 μg/ml; chloramphenicol, 20 μg/ml for *E. coli* and 10 μg/ml for GAS; and kanamycin, 30 μg/ml. In certain studies, THY was supplemented with $FeCl_3$, $MnCl_2 \cdot 4H_2O$, or deferoxamine mesylate (Sigma), as indicated. For H_2O_2 experiments, fresh working solutions (0.1 to 1 M) were prepared in water from a 10 M stock (Sigma).

DNA and RNA techniques. Plasmid pGEM-T (Promega) is a linear *E. coli* vector used for cloning of PCR products; pJL1055 is a temperature-sensitive *E. coli*-Gram-positive shuttle vector used for mutagenesis in *Streptococcus* (21). Chromosomal DNA isolation and GAS electroporation were performed as described previously (22). Total GAS RNA was isolated using the RNeasy minikit (Qiagen) from bacterial lysates obtained by shaking bacteria with glass beads on a dental amalgamator (22).

PCR and qRT-PCR. Primers used are shown in Table S1 in the supplemental material and were designed on the basis of the M-type 3 GAS strain MGAS315 or M-type 1 GAS strain SF370 genome sequences (4, 16). Quantitative reverse transcriptase PCR (qRT-PCR) was performed on an ABI PRISM 7300 sequence detection system (Applied Biosystems) using the QuantiTect SYBR green RT-PCR kit (Qiagen). Relative expression levels were calculated by the $\Delta\Delta C_T$ (C_T stands for threshold cycle) method described previously (22). Expression levels were normalized to *recA* (*spyM3_1800*) for studies in the absence of H_2O_2 and to *gyrA* (*spyM3_0810*) encoding DNA gyrase subunit A for studies with H_2O_2. Expression of both genes remained unaffected by *perR* mutation, while *gyrA* expression did not change in peroxide.

Microarray procedures and data analyses. The GAS DNA microarray represents 1,788 open reading frames (ORFs), including 1,695 ORFs of M-type 1 GAS strain SF370, in addition to 71 M-type 18 and 21 M-type 3 specific ORFs (21). cDNA synthesis and labeling, microarray hybridizations, and data analyses were performed as described previously (22). The wild-type strain 003Sm and *perR* mutant strain 003Sm*perR*Δ were grown to mid-exponential (ME) phase (A_{600} of 0.25) or late exponential (LE) phase (A_{600} of 0.6) at which point they were challenged with H_2O_2 (final concentration of 0.5 mM) for 15 min at 37°C or with water as a control. For each strain, total bacterial RNA was extracted from three or four independent H_2O_2- or water-treated control cultures, pooled, and used for cDNA synthesis and labeling. RNA samples to be compared were converted to cDNA, fluorescently labeled with Cy3 or Cy5 in direct (Cy3-Cy5) and dye swap (Cy5-Cy3) labeling reactions to correct for dye-dependent variation of labeling efficiency, and cohybridized on the arrays. Transcriptome comparisons were performed between treated and control wild-type strain 003Sm or *perR* mutant strain 003Sm*perR*Δ. Statistical significance of the difference in mean fluorescence intensity calculated for each gene in the cDNA samples compared was determined by an unpaired 2-tailed Student's *t* test. Genes whose relative expression was equal or exceeded 2.0-fold and had *P* values of ≤0.01 were considered differentially expressed. Validation of the microarray data was performed by qRT-PCR using a minimum of two independent RNA samples obtained from peroxide-treated and untreated cultures of GAS grown to ME or LE phase.

Complementation and site-directed mutagenesis of PerR. For complementation of strain 003Sm*perR*Δ, wild-type *perR* was introduced into the native locus on the mutant chromosome by homologous recombination (21). A DNA fragment encompassing the full-length coding sequences of *spyM3_0146* and *perR* (*spyM3_0147*) and the 3′-end sequence of *spyM3_0148* transcribed in the opposite orientation was amplified using primers 0146-F (F for forward) (BamHI) and 0148-R (R for reverse) (EcoRV). This fragment was cloned into BamHI/EcoRV double-digested pJL1055 to obtain plasmid pJL*perR*. The construct was introduced into strain 003Sm*perR*Δ by electroporation and was inserted into the chromosome upstream of *perR* by homologous recombination, generating *perR*Δ::WT (WT stands for wild type) strain. To obtain PerR mutants $PerR_{H44A}$ and $PerR_{C104S}$, the QuikChange II site-directed mutagenesis kit (Agilent Technologies) was used as instructed with plasmid pJL*perR* as the template and primer pair perR-H44A-F/perR-H44-R and perR-C104S-F/perR-C104S-R, respectively. The derivative plasmids were introduced into mutant strain 003Sm*perR*Δ by electroporation and then inserted into the chromosome by homologous recombination as described for wild-type *perR* to generate *perR*Δ::H44A and *perR*Δ::C104S strains. The presence of wild-type *perR* and *spyM3_0146* sequences in the *perR*Δ::WT strain or wild-type *spyM3_0146* and the mutations in the *perR*Δ::H44A and *perR*Δ::C104S strains were confirmed following sequencing of PCR products encompassing the two genes from each strain.

GAS protein preparation and Western blotting. Total GAS protein preparations were obtained from cultures grown to ME phase using a combination of mutanolysin and lysozyme (22). Proteins were analyzed by SDS-PAGE under reducing conditions using 10% NuPAGE Bis-Tris gels (Invitrogen). For Western blots, proteins were transferred to nitrocellulose membranes and blocked in phosphate-buffered saline (PBS) containing 5% milk (PBS–5% milk) (Difco Laboratories). Anti-PerR rabbit serum (21) was added to the membranes at 1:5,000 in PBS–5% milk for 1 h, and the membranes were incubated with peroxidase-conjugated secondary antibody (GE Healthcare). Membrane development was carried out using the SuperSignal West Pico chemiluminescent substrate (Thermo Scientific). To confirm equal amounts of loaded proteins, samples were analyzed by SDS-PAGE and stained with Coomassie blue R-250.

Expression and purification of recombinant wild-type and mutant PerR. The *perR* sequence without the start codon was amplified using primer pair perR-F (PshAI)/perR-R (HindIII) and was cloned downstream of the glutathione *S*-transferase (GST) coding sequence in PshAI/HindIII double-digested plasmid pET41a (EMD Chemicals) to generate pET41-*perR*. Overexpression of the ~49-kDa recombinant GST-PerR fusion protein, or of GST protein from empty vector as a control, was achieved in *E. coli* BL21(DE3) using isopropyl-β-D-thiogalactopyranoside (IPTG) induction for 90 min in LB broth supplemented with 10 μM $ZnCl_2$ and 40 μM $FeSO_4$. Cell extracts were obtained by French press lysis, and purification was achieved using GST-binding resin (EMD Chemicals) as instructed by the manufacturer. To obtain GST-$PerR_{H44A}$ and GST-$PerR_{C104S}$ recombinant protein mutants, the QuikChange II site-directed mutagenesis kit (Agilent Technologies) was used with plasmid pET41-*perR* as the template and with primer pairs perR-H44A-F/perR-H44A-R and perR-C104S-F/perR-C104S-R, respectively. Expression and purification of the two mutant proteins was performed as described for GST-PerR. For certain preparations of GST-PerR, purification was performed in the presence of 1 to 10 mM EDTA. All purified proteins were obtained at higher than 95% purity, as determined by SDS-PAGE analysis. GST-PerR concentrations were determined using a NanoDrop 1000 spectrophotometer (Thermo Scientific) and an extinction coefficient of 55280 M^{-1} cm^{-1} at 280 nm.

Metal content analyses of culture media and recombinant PerR. The metal content of THY broth was determined by inductively coupled plasma mass spectrometry (ICP-MS) using a Thermo Fisher Scientific X-Series instrument at the Department of Earth and Planetary Sciences at Harvard University. In similar analyses, metal bound to purified recombinant wild-type and mutant GST-PerR variant proteins was determined. For these measurements, 4 to 5 mg of each purified product, including recombinant GST expressed from an empty vector as a control, was diluted at ~0.4 mg/ml and analyzed in buffer with a final composition of 20 mM Tris (pH 8.0), 2% glycerol, 3 mM glutathione, and 0.02% Tween 20. For both THY broth and purified proteins, two or three independent samples were analyzed for eight metal ions (calcium, cobalt, copper, iron, magnesium, manganese, nickel, and zinc), and the averages of these determinations were reported.

Electrophoretic mobility shift assays. Binding of purified recombinant GST-PerR or GST-$PerR_{H44A}$ to promoter fragments was examined as described previously (21). In brief, GST-PerR or GST-$PerR_{H44A}$ recombinant protein was mixed with DNA at a final concentration of 6 μM or 50 nM, respectively.

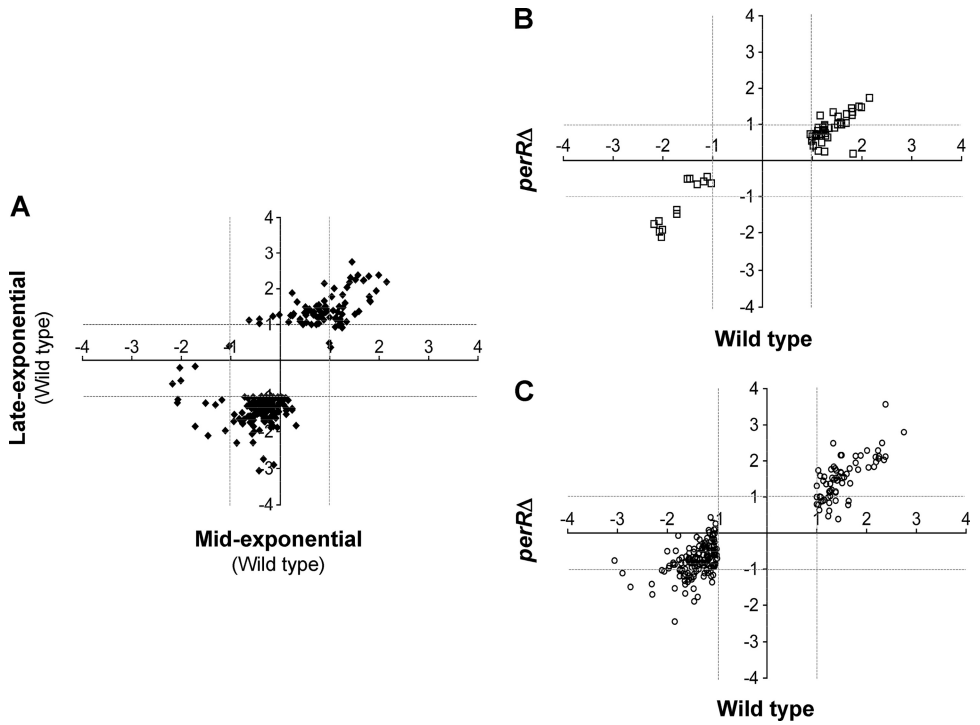

FIG. 1. Transcriptome changes elicited by H_2O_2 in GAS. (A) Gene expression changes ($\log_2$) in wild-type strain 003Sm following H_2O_2 challenge at mid-exponential and late-exponential phase growth. (B and C) Comparison of gene expression changes ($\log_2$) between wild-type and *perR* mutant strain 003Sm*perR*Δ at each of the two growth phases. Data for the wild type and mutant are shown on the *x* axis and *y* axis, respectively. Broken vertical and horizontal lines represent 2-fold change in expression ($\log_2 = 1$) that was used as a threshold value for regulated genes.

Reactions were allowed to proceed for 15 min at room temperature, and then the proteins were resolved on 6% native polyacrylamide DNA retardation gels (Invitrogen) and stained with ethidium bromide. The ~300-bp *pmtA* promoter fragment carrying a fully conserved Per box was obtained by PCR using primer pair GS-1093-F/GS-1093-R. Negative-control reaction mixtures contained purified recombinant GST or a negative-control (*gyrA*) promoter fragment obtained with primer pair GS-gyrA-F/GS-gyrA-R (see Table S1 in the supplemental material).

Sequence databases and analyses tools. Assignment of gene function was obtained from the National Center for Biotechnology Information (NCBI) and the Kyoto Encyclopedia of Genes and Genomes Sequence Similarity Database (KEGG SSDD) (31). Protein sequence alignments were performed using ClustalW2 (35). Searches for Per box-like sequences on promoters were carried out using the PredictRegulon server (67).

Microarray data accession number. The primary microarray data have been submitted to the ArrayExpress database of the European Bioinformatics Institute under accession number E-MTAB-646.

RESULTS

Genome-wide GAS responses to peroxide. Wild-type strain 003Sm and isogenic *perR* mutant strain 003Sm*perR*Δ were grown to mid-exponential (ME) and late exponential (LE) phase in THY broth, and bacteria were challenged with a sublethal concentration of H_2O_2 (0.5 mM) for 15 min at 37°C. Experimental conditions were chosen on the basis of pilot wild-type and *perR* mutant cultures challenged with peroxide concentrations ranging from 0.2 to 10 mM (see Fig. S1 in the supplemental material). The 0.5 mM final peroxide concentration used for microarray analyses showed no effect on growth during LE phase and a moderate effect during ME phase, while no significant loss of cell viability was evident in either growth phase as determined by quantitative culture following peroxide challenge. Total RNA samples were collected from untreated control or peroxide-treated wild-type or mutant bacteria, and cDNA was generated and hybridized with GAS genomic DNA microarrays (21). Transcriptome changes in wild-type and *perR* mutant bacteria were identified by comparing the levels of gene expression in bacterial strains grown in the presence of peroxide with those in untreated samples of each strain. Changes induced by H_2O_2 in both strains constituted PerR-independent loci, whereas responses identified exclusively in wild-type bacteria constituted PerR-dependent loci.

A total of 237 genes, including 40 encoding hypothetical proteins, were differentially regulated (≥2-fold change, $P \leq 0.01$) in wild-type bacteria treated with peroxide at ME and/or LE phase: 84 genes were upregulated, and 153 were downregulated (Fig. 1A; see Table S2 in the supplemental material). Of these genes, 51 were regulated at the ME phase, whereas 214 genes were regulated at the LE phase or both growth phases. Interestingly, the majority of genes identified at the ME phase were upregulated (38 of 51, or 75%), whereas approximately two-thirds of the genes identified at the LE phase were downregulated in response to peroxide challenge (Fig. 1B and C).

qRT-PCR verification of transcriptome events. Validation of the microarray data was carried out by quantitative reverse transcriptase PCR (qRT-PCR) analyses of RNA samples obtained from both wild-type and *perR* mutant bacteria exposed to H_2O_2 independent from those used for microarray studies (Table 1). A total of 40 genes representing ~30 putative or known operons that include approximately 80 genes were ex-

TABLE 1. qRT-PCR analysis of GAS responses to H_2O_2

SPy no.[a]	Gene	Function[b]	Microarray/qRT-PCR[c]		Growth[d]
			Wild type	*perR*Δ mutant	
PerR-dependent genes					
0092 (*0069*)	*adcR*	Putative transcriptional repressor	+1.8/+2.3	+1.1/1.0	ME
0094 (*0071*)	*adcB*	Zinc/manganese ABC transporter	+2.4/+1.7	+1.2/1.0	ME
0454 (*0319*)	*mtsB*	Iron ABC transporter	−2.7/−2.3	−1.4/−2.2[f]	ME
1198 (*0840*)		Putative transcriptional repressor	+3.5/+6.0	+1.1/−1.3	ME
0016 (*0013*)		Putative amino acid permease	−3.5/−2.2	−1.4/−1.5	LE
0295 (*0217*)	*oppC*	Oligopeptide permease	−3.4/−2.6	−1.7/−1.4	LE
0416 (*0298*)	*prtS*	Interleukin 8 protease	−3.7/−2.4	−1.7/−1.2	LE
0740 (*0482*)	*sagC*	Streptolysin S-associated ORF	−2.3/−1.6	−1.1/1.0	LE
1618 (*1363*)	*cysM*	Putative *O*-acetylserine lyase	+2.7/1.0[e,f]	+1.3/−1.3	LE
1791 (*1557*)	*siaD*	Putative ABC transporter	−2.9/−1.9	−1.5/−1.1	LE
1796 (*1560*)	*shp*	Heme/ferrichrome-binding protein	−3.3/−2.0	−1.6/−1.1	LE
1922 (*1658*)	*lacB2*	Galactose-6-phosphate isomerase	−8.3/−2.4	−1.7/−1.2	LE
1923 (*1659*)	*lacA2*	Galactose-6-phosphate isomerase	−6.7/−3.7	−2.8/−1.5	LE
2110 (*1794*)	*nrdD*	Ribonucleoside triphosphate reductase	−4.0/−4.4	−1.4/−1.7	LE
PerR-independent genes					
n/a (*0097*)	*nra*	Pilus transcriptional repressor	ND/+4.4	ND/nd	ME
n/a (*0098*)	*cpa*	Pilus ancillary protein	ND/+6.8	ND/nd	ME
n/a (*0100*)	*fctA*	Pilus major subunit	ND/+7.1	ND/nd	ME
n/a (*0101*)	*srtC2*	Sortase B family	+2.6/+3.7	+2.0/nd	ME
n/a (*0102*)	*fctB*	Pilus minor subunit	ND/+5.8	ND/nd	ME
n/a (*0103*)	*msmR*	Pilus transcriptional activator	ND/+6.6	ND/nd	ME
0146 (*0113*)	*sloR*	Putative regulatory protein	−4.1/−6.7	−4.4/nd	ME
0290 (*0212*)	*sufB*	Putative Fe-S cluster assembly protein	+3.0/+4.0	+2.0/nd	ME
1134 (*0792*)	*proX*	L-Proline glycine betaine ABC transport	+2.5/+1.9	+1.9/nd	ME
1212 (*0852*)	*cls*	Cardiolipin synthetase	+3.5/+3.5	+2.4/nd	ME
1214 (*0854*)	*lplA*	Putative lipoate-protein ligase	+4.4/+3.8	+3.3/nd	ME
1217 (*0857*)	*gcvH*	Glycine cleavage system H protein	+3.2/+5.2	+2.4/nd	ME
1406 (*1071*)	*sodA*	Superoxide dismutase	+2.2/+3.5	+2.4/nd	ME
1835 (*1586*)	*trx*	Putative thioredoxin	+2.3/+1.6	+1.8/nd	ME
1849 (*1596*)	*pfl*	Putative pyruvate formate lyase	−3.3/−9.2	−2.6/nd	ME
1856 (*1601*)	*norA*	Putative antibiotic resistance protein	−4.2/−3.7	−3.2/nd	ME
2080 (*1771*)	*ahpF*	Alkyl hydroperoxide reductase	+2.1/+3.2	+1.8/nd	ME
0100 (*0077*)		Putative DNA-binding protein	+5.2/+8.5	+4.4/nd	LE
0165 (*0128*)	*nga*	NAD glycohydrolase	−3.0/−3.6	−2.1/nd	LE
0386 (*0283*)	*fhuA*	Heme/ferrichrome ABC transporter	−3.0/−2.6	−2.5/nd	LE
0412 (*0296*)	*exoA*	Putative 3′-exo-DNase	+2.8/+3.2	+4.4/nd	LE
0454 (*0319*)	*mtsB*	Iron/manganese ABC transporter	−4.3/−2.5	−2.0/−2.0	LE
0813 (*0546*)	*gor*	Glutathione reductase	+2.4/+3.7	+1.9/nd	LE
0914 (*0629*)		Hypothetical protein	+5.2/+7.1	+11.8/nd	LE
1131 (*0790*)		Na^+-driven multidrug efflux pump	+4.7/+3.5	+4.9/nd	LE
1206 (*0847*)		Putative ABC transporter	−4.9/−6.8	−3.2/nd	LE
1219 (*0859*)		Putative trimethylamine dehydrogenase	+6.7/+3.3	+7.0/nd	LE
1607 (*1355*)	*recX*	RecA function regulator	+5.0/+3.5	+5.6/nd	LE
1680 (*1464*)		Putative transcriptional regulator	+3.7/+3.6	+4.4/nd	LE
1681 (*1465*)		Putative NADH peroxidase	+2.2/+1.6	+3.0/nd	LE
1816 (*1570*)	*scrB*	Putative sucrose-6-phosphate hydrolase	+2.8/+1.4[e]	+3.2/nd	LE
1825 (*1577*)	*uvrA*	Excinuclease ABC subunit A	+2.6/+2.6	+3.3/nd	LE
2162 (*1818*)	*cadD*	Putative cadmium resistance protein	−2.6/−1.6[e]	−1.6/−1.4	LE

[a] The *SPy* numbers of the M-type 1 strain SF370 (16) are shown. The *spyM3* numbers of the M-type 3 strain MGAS315 (4) are shown in parentheses. n/a, nonapplicable.

[b] NCBI or KEGG annotation.

[c] Fold change expression in the wild type or *perR*Δ mutant following challenge with H_2O_2 (0.5 mM) versus H_2O control. Data obtained by microarray and qRT-PCR analyses are shown before and after the slashes, respectively. nd, not done; ND, not detected due to lack of sequence homology between M-type 3 strain 003Sm and M-type 1 sequences on microarrays.

[d] ME, mid-exponential phase; LE, late exponential phase.

[e] Regulation not confirmed by qRT-PCR.

[f] PerR dependence not confirmed by qRT-PCR.

amined. These genes represented both moderately and highly up- and downregulated PerR-dependent and -independent genes identified by microarray. We observed a high correlation ($R = 0.92$) between qRT-PCR results and microarray data (see Fig. S2 in the supplemental material). Additional qRT-PCR analyses examined independent samples obtained 5 and 15 min after challenge with 0.2, 0.5, or 1 mM H_2O_2 in order to evaluate both the strength and kinetics of peroxide-elicited GAS responses. These analyses including 11 or more genes showed dose-dependent responses in peroxide-treated bacteria and

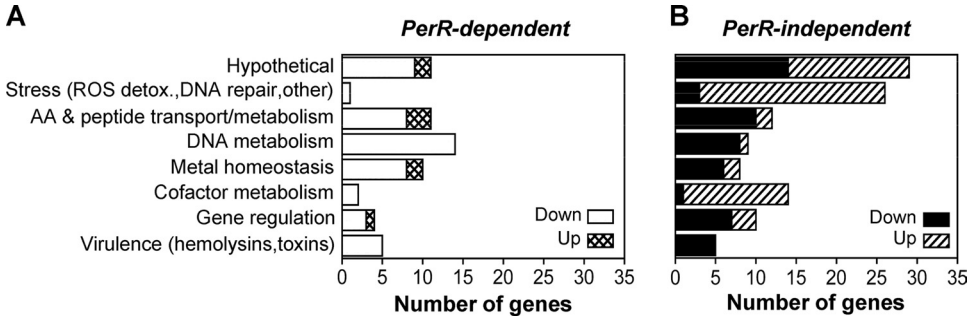

FIG. 2. PerR-dependent (A) and PerR-independent (B) GAS responses elicited by H_2O_2. The numbers of downregulated and upregulated genes in each of eight main categories are shown. Note that PerR-dependent genes mainly encode DNA metabolism, metal homeostasis, and amino acid (AA)/peptide transport. The majority of genes with functions in DNA repair, ROS detoxification (detox.), cofactor metabolism and gene regulation as well as genes encoding hypothetical proteins are PerR independent.

suggested optimal regulation at 15 min versus 5 min (data not shown).

Responses to H_2O_2 are partially dependent on PerR. PerR-regulated responses were identified as transcriptome changes in wild-type bacteria that were not observed in the *perR* mutant. To ensure stringent selection of PerR-dependent loci, regulated genes in wild-type bacteria (≥2-fold change, $P \leq 0.01$) that showed a similar regulation trend (≥1.6-fold, $P \leq 0.05$) in the *perR* mutant were not considered PerR dependent. Moreover, peroxide-induced regulation of several genes that showed dependence on PerR in microarrays was verified by qRT-PCR (Table 1). These genes included certain loci for which PerR dependence was not clear by microarray. On the basis of the results of both analyses, 76 of 237 genes (32%) including 11 genes encoding hypothetical proteins were identified as PerR dependent. The great majority of these genes (67 of 76) were downregulated by PerR (directly or indirectly) at LE phase growth and mainly encoded products involved in purine and deoxyribonucleotide synthesis, amino acid/oligopeptide synthesis and transport, and heme acquisition among others (Fig. 2A; see Table S2 in the supplemental material). Upregulated loci encoded proteins involved in Mn^{2+}/Zn^{2+} import and methionine uptake but also included a putative transcriptional regulator (*SPy1198*) that was among the most highly regulated PerR-dependent loci (Table 1 and Fig. 3B).

PerR-independent responses to peroxide encompassed 161 genes (68% of total) of which 86 were downregulated and 75 were upregulated (Fig. 2B). Repressed genes encoded proteins with functions similar to those in PerR-mediated responses, including iron and heme/ferrichrome uptake, amino acid/peptide transport and metabolism, pyrimidine synthesis, as well as a significant number of hypothetical proteins. Upregulated genes showed very little or no overlap in function with PerR-dependent responses and encoded proteins involved in DNA damage repair, ROS detoxification, lipoic acid protein modification, iron-sulfur cluster (Fe-S) synthesis/repair, pilus biosynthesis, and almost all (15 of 17) upregulated hypothetical proteins.

Overall, the greatest numbers of PerR-dependent loci were identified in the DNA metabolism, metal homeostasis, and amino acid/peptide transport categories, with regulation of over half of the genes in these three groups (35 of 64, or 55%) showing dependence on PerR (Fig. 2). These data demonstrate a significant, but also nonexclusive, role of PerR in GAS responses to peroxide stress.

DNA damage repair, ROS detoxification, and other stress responses. All but one of 27 genes in the category of DNA damage repair, ROS detoxification, and other stress responses exhibited PerR-independent regulation, with the great majority (23 of 27) upregulated in the presence of peroxide (Fig. 2). Highly upregulated genes encoded proteins with predicted functions in DNA repair, such as excinuclease subunits A (*uvrA*, *SPy1825*) and C (*uvrC*, *SPy1068*) involved in base excision repair, exo-DNase A (*exoA*, *SPy0412*) implicated in oxidative damage repair in *Bacillus subtilis* (28), and MutY (*SPy1833*) that is a putative adenine glycosylase that removes misincorporated adenine opposite from 8-oxo-7,8-dihydroguanine, a toxic product resulting from oxidative DNA damage (42). *recX* (*SPy1607*) encoding a regulator of recombinase A (*recA*) function was strongly upregulated (~5-fold) in PerR-independent fashion, while upregulation of *recA* itself was 2-fold in peroxide-treated GAS. RecA and RecX, in addition to UvrA and UvrC, are important components of the SOS response in several bacterial species required for repair of DNA damage caused by ROS and other chemical or physical agents (13, 66).

Additional upregulated genes encoded peroxide and other ROS detoxifying enzymes, such as alkyl hydroperoxidase/alkyl hydroperoxide reductase AhpC/AhpF (*SPy2079-SPy2080*), a putative NADH peroxidase (*npr*, *SPy1681*), superoxide dismutase (*sodA*, *SPy1406*) and glutathione reductase (*gor*, *SPy0813*). The latter converts oxidized glutathione (GSSG) to its reduced form (GSH) that can itself reduce oxidized thiol groups directly or contribute to peroxide detoxification indirectly through the action of glutathione peroxidase, which degrades H_2O_2 to water with concomitant oxidation of GSH (6). Upregulation of *sodA* was not surprising, as it is also upregulated by peroxide in *B. subtilis* (48) and has been reported to contribute to peroxide resistance in streptococci by counteracting oxidative DNA damage (54).

A five-gene locus with a putative role in Fe-S assembly was also activated in the presence of peroxide (Fig. 3F). While certain bacteria encode more than one Fe-S synthesis system (Isc, Nif, Suf), streptococci encode a single system comprised mainly of Suf-like enzymes (SufC/SufD/SufS/SufB) (55). Upregulation of a rhodanese-related sulfurtransferase (*SPy0915*),

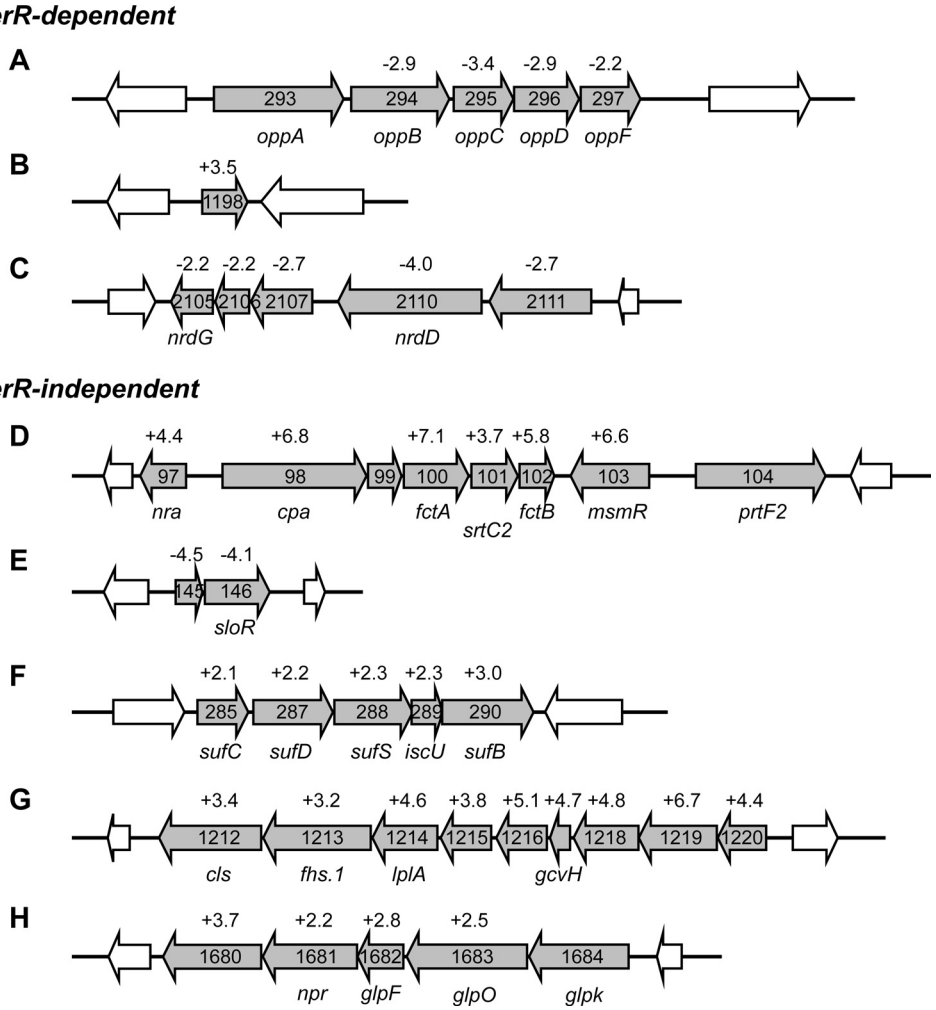

FIG. 3. Chromosomal organization and regulation levels of GAS loci in peroxide. (A to C) PerR-dependent loci encompassing the oligopeptide permease locus (A), a putative transcriptional regulator (B), and a deoxynucleoside triphosphate (dNTP) synthesis locus (C) are shown. (D to H) PerR-independent loci include the pilus biosynthesis operon and regulator genes in FCT-3 region (D), two independent loci involved in Fe-S (F) and other cofactor (lipoic acid) metabolism (G), and two loci encoding putative regulators SloR (*SPy0146*) (E) and *SPy1680* (H). The gene numbers in each panel represent ORFs of M-type 1 GAS strain SF370 (16), except for panel D, which shows ORFs of M-type 3 GAS strain MGAS315 (4). The numbers above genes indicate relative expression levels (fold change) in wild-type strain 003Sm treated with peroxide as obtained in microarray studies, except for FCT-3 regulation (panel D) that was characterized by qRT-PCR.

which is thought to have a SufS-like function and to contribute to oxidative stress defenses, was also detected (32).

DNA metabolism. Regulation of a total of 23 genes in the DNA metabolism category was detected exclusively at LE phase growth, and all but one was repressed in peroxide. It was striking that 14 of 23 genes were PerR dependent and included mostly purine (*purM*, *purN*, *purE*, *purB*, and *guaB*) and deoxyribonucleotide synthesis loci. The latter were clustered in a single operon or two adjacent potential operons (Fig. 3C) encompassing *nrdG* (*SPy2105*) and *nrdD* (*SPy2110*), which encode putative class III ribonucleotide reductases involved in deoxyribonucleotide synthesis under anaerobic conditions (19). PerR-independent loci encoded DNA replication machinery components (*dnaA*, *dnaN*, *dnaX*, *topA*, and *priA*) as well as pyrimidine biosynthesis (*pyrB*, *pyrF*, and *pyrE*).

Amino acid/peptide transport and metabolism. The amino acid/peptide transport and metabolism category encompassed mostly repressed genes (18 of 23 total) that included the oligopeptide permease operon *oppABCDF* (52) and three ABC transport loci with predicted function in polar amino acid transport (*SPy0276-SPy0277*, *SPy1274-SPy1276*, and *SPy1506-SPy1507*). Eight repressed genes including the *opp* operon were regulated in a PerR-dependent manner. Of the five upregulated genes, *SPy0320-SPy0321* are PerR dependent and encode a putative methionine ABC transporter, while *SPy1990-SPy1991* seem to encode a protein(s) involved in aromatic amino acid biosynthesis. Among amino acids, methionine is highly reactive with ROS; therefore, increased uptake would counteract peroxide-induced protein damage.

Metal homeostasis and transport. Twelve of 18 genes represented the three known iron and heme acquisition systems of GAS: the MtsABC iron transport system (*SPy0453*, *SPy0454*, and *SPy0456*), the FhuGBDA or FtsDCBA (*SPy0383-SPy0386*) heme/ferrichrome transport system, and Shr/Shp/SiaABCD

(*Spy1791*, *SPy1793-SPy1796*, and *SPy1798*; *siaABC* is also known as *htsABC*) involved in hemoglobin acquisition (3, 24, 30, 39, 40, 62). All three operons were repressed in peroxide with PerR mediating repression of at least the Shr/Shp/SiaABCD gene locus, as confirmed by qRT-PCR (Table 1). Repression of *mtsABC* at ME phase growth was also suggested to be PerR dependent by microarray analysis. This result could be verified by qRT-PCR in the RNA preparations used for microarrays, but it could not be reproduced using independent RNA preparations; therefore, the role of PerR in *mtsABC* repression remains unclear. Of the four upregulated genes, three represented AdcRCB (*SPy0092-SPy0094*), a transport complex linked to Mn^{2+}/Zn^{2+}import in streptococci (14, 41). Upregulation of this locus was moderate but consistently dependent on PerR at ME phase (Table 1).

Cofactor metabolism. Similar to the first category (DNA damage repair, ROS detoxification, and other stress responses), the majority of genes in the cofactor metabolism category (14 of 16) were upregulated by peroxide in a PerR-independent manner. Nine genes were activated to similar levels at both ME and LE growth phase and seemed to be organized in an operon (*SPy1212-SPy1220*) that included some of the most highly upregulated genes in the peroxide stimulon (Fig. 3G). While several genes in this locus are genes encoding hypothetical proteins, *SPy1214* encodes a predicted lipoate-protein ligase (*lplA*) that uses exogenous lipoic acid to lipoylate components of keto acid dehydrogenase complexes (20, 47, 61), such as the E2 subunits of pyruvate dehydrogenase and protein H of the glycine cleavage system, with protein H encoded by *SPy1217* (*gcvH*) in the same operon. Lipoic acid (6,8-thiooctanoic acid), a disulfide-containing cofactor, is essential for the decarboxylation activity of these complexes (61), but it has also been reported to contribute to bacterial defenses against oxidative stress (8).

Interestingly, the last gene in this locus (*cls*, *SPy1212*) encodes a synthetase involved in production of cardiolipins, anionic glycerophospholipids that have been reported to be upregulated under osmotic stress (57). Although cardiolipins are not essential for GAS growth under standard culture conditions (58), *cls* activation in peroxide could be important for repair of ROS-inflicted membrane damage or for increasing cardiolipin membrane levels that may enhance bacterial fitness under oxidative stress. Consistent with increased cardiolipin synthesis, *glpF* (*SPy1682*) and *glpO* (*SPy1683*) involved in glycerol uptake and glycerophospholipid metabolism were also upregulated in the presence of peroxide (Fig. 3H).

Pilus biosynthesis. The microarray data initially suggested upregulation of *srtC2* (*spyM3_0101*) encoding a type B sortase that is required for pilus assembly in GAS (49). This enzyme is expressed from the pilus biosynthesis operon, also encoding three pilus structural proteins (*fctA*, *fctB*, and *cpa*), which is part of the fibronectin-binding, collagen-binding, T antigen (FCT) region in the GAS chromosome (Fig. 3D). The FCT locus is conserved in GAS strains of M-types 3, 5, 18, and 49 (FCT-3), but it shows variable gene content and poor sequence homology with FCT regions from other strains, such as M-type 1 GAS representing FCT-2 (15, 46). *srtC2* regulation was detectable in M-type 3 strain 003Sm, because our microarrays carry probes for the highly homologous *srtC2* from M-type 18 GAS (*spyM18_0129*) (60), whereas regulation of the pilus structural genes was not detectable, since the microarrays contained probes specific to M-type 1 GAS. To further assess pilus operon regulation in strain 003Sm, we designed primers for the three structural genes and *srtC2* based on FCT-3 sequences from M-type 3 GAS (4) and measured expression in response to peroxide by qRT-PCR. As shown in Table 1, these studies confirmed upregulation of the sortase and showed 6- to 7-fold increased expression of the three structural genes.

PerR complementation restores PerR-regulated gene expression. To verify the transcriptome events mediated by PerR in response to peroxide, as well as those identified in previous studies by comparing the *perR* mutant transcriptome with the wild-type transcriptome in the absence of ROS (7, 21), PerR-dependent regulation was evaluated both in the presence and absence of peroxide in a complemented *perR* deletion mutant strain 003Sm*perR*Δ. Complementation was achieved by introducing wild-type *perR* into its native locus on the chromosome using plasmid pJL*perR* and a homologous recombination strategy identical with that used for constructing the original deletion mutant. The resulting strain designated the *perR*Δ::WT strain expressed wild-type *perR* mRNA levels and fully restored PerR protein expression, as indicated, respectively, by qRT-PCR and Western blot analyses using PerR antiserum against cell lysates of the *perR*Δ::WT strain as well as of the wild type and *perR* deletion mutant (*perR*Δ) as controls (Fig. 4). PerR regulation in the *perR*Δ::WT strain and in control wild-type and *perR*Δ cultures was then assessed by qRT-PCR analyses of RNA samples isolated from bacteria grown to ME phase with or without subsequent H_2O_2 challenge. PerR function in peroxide was evaluated by comparing expression levels of *SPy1198* in peroxide-treated versus untreated controls, whereas PerR regulation in the absence of peroxide was determined by comparing expression of *pmtA* (*SPy1434* or *spyM3_1093*) and *adcA* (*SPy0714* or *spyM3_0466*) that were previously identified as two PerR-repressed genes in the absence of stress (7, 21). *SPy1198* was chosen as a marker for peroxide-mediated gene expression, because it represents the most strongly regulated PerR-dependent gene following qRT-PCR verification and encodes a predicted transcriptional regulator that could further influence PerR-mediated adaptive responses to ROS. These studies showed clear restoration of PerR function in the *perR*Δ::WT strain, leading to ~5-fold upregulation of *SPy1198* in the presence of peroxide versus ~6-fold in the wild-type parent strain (Fig. 5A) and repression of both *pmtA* and *adcA* to wild-type levels in the absence of peroxide (Fig. 5B). As expected, derepression of *pmtA* and *adcA* in the absence of stress and no *SPy1198* upregulation in peroxide were recorded in the *perR* deletion mutant.

Mutagenesis of predicted metal-binding sites abrogates PerR function. In the well-characterized *Bacillus* system, PerR binds one Fe^{2+} (or Mn^{2+}) atom at a regulatory site encompassing a histidine (H37) as well as four other amino acid residues, and one Zn^{2+} atom at a structural site encompassing four cysteines, including C96 (37, 38). Eight of these nine residues are conserved between GAS and *Bacillus* PerR. Fe^{2+}-bound PerR is responsive to peroxide, as Fe^{2+} is oxidized to Fe^{3+} with concomitant oxidation of H37 to oxo-H37 due to Fenton chemistry, leading to the loss of PerR regulatory (repressor) function. In contrast, Mn^{2+}-bound PerR is much less

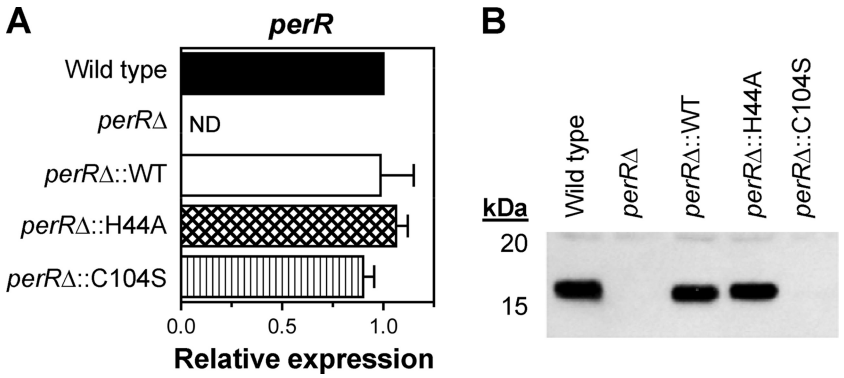

FIG. 4. Complementation analyses of *perR* deletion mutant strain 003Sm*perR*Δ expressing wild-type PerR (*perR*Δ::WT strain) or one of two mutant variants $PerR_{H44A}$ (*perR*Δ::H44A strain) and $PerR_{C104S}$ (*perR*Δ::C104S strain). (A) PerR mRNA levels in each strain relative to the wild-type parent control, as determined by qRT-PCR. Data represent means plus standard deviations (error bars) obtained from at least three independent RNA preparations for each strain. ND, not detected. (B) Western blot analysis of total protein preparations obtained from strains shown in panel A using PerR antiserum.

sensitive to oxidation and retains DNA binding in high peroxide concentrations (38, 64).

To gain insight into the mechanism of PerR function in GAS, we studied two additional *perR* deletion mutant-derived strains complemented with PerR variants carrying single point mutations at H44 or C104 corresponding to H37 and C96 of *Bacillus*. The wild-type *perR* gene on the pJL*perR* plasmid was mutated at H44 to alanine and at C104 to serine, generating plasmids pJL$perR_{H44A}$ and pJL$perR_{C104S}$, respectively. Each of the two *perR* mutant variants was introduced into the *perR*Δ chromosome by homologous recombination as described previously for wild-type *perR* to produce *perR*Δ::H44A and *perR*Δ::C104S strains. The levels of PerR mRNA and protein as well as PerR-regulated gene expression were then compared to those in the wild-type *perR*-complemented strain (*perR*Δ::WT strain) by qRT-PCR and Western blot analyses. As shown in Fig. 4A, *perR* transcript levels of the two mutants were restored to the levels of the wild type, similar to the result obtained for the *perR*Δ::WT strain. PerR protein expression in the *perR*Δ::H44A strain was indistinguishable from that of the wild type, but it was not detectable in the *perR*Δ::C104S strain (Fig. 4B) despite wild-type mRNA levels detected by qRT-PCR. Longer exposure of Western blots revealed very low $PerR_{C104S}$ expression levels, indicating that lack of detection by anti-PerR serum was not due to altered conformation of the mutant protein. This explanation was supported by the finding that the mutant protein could be detected by the same antiserum as a recombinant fusion protein to glutathione *S*-transferase described below (data not shown). Consistent with rapid degradation of $PerR_{C104S}$, regulation of *SPy1198* in the presence of peroxide and of *pmtA* and *adcA* in its absence remained unchanged in the *perR*Δ::C104S strain compared to the *perR*Δ strain. Moreover, the complete loss of *pmtA* and *adcA* repression in the absence of peroxide as well as loss of *SPy1198* upregulation in peroxide-treated bacteria was also observed in the *perR*Δ::H44A strain, even though $PerR_{H44A}$ expression was at wild-type levels (Fig. 5). These results show the requirement of both H44 and C104 for PerR function in GAS and indicate metal-binding sites analogous to those reported in *Bacillus*.

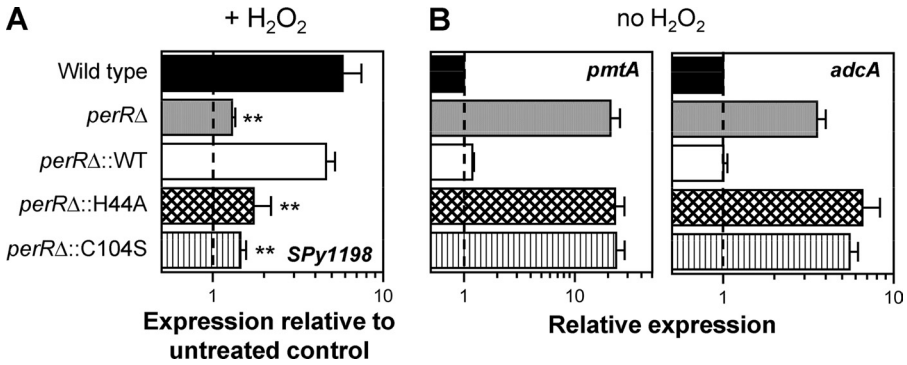

FIG. 5. PerR-regulated gene expression in mutant strain 003Sm*perR*Δ expressing wild-type PerR or one of two mutant variants, $PerR_{H44A}$ and $PerR_{C104S}$. (A) Regulation of *SPy1198* after peroxide challenge, as determined by qRT-PCR. Relative expression equal to 1, indicated by the broken line, represents no change in expression in the presence of peroxide compared to expression in untreated control cultures. **, $P \leq 0.009$ for comparison of *SPy1198* upregulation in *perR*Δ::WT versus *perR*Δ, *perR*Δ::H44A, or *perR*Δ::C104S (Student's *t* test). (B) Regulation of *pmtA* and *adcA* in the absence of peroxide, as determined by qRT-PCR. The level of expression in the wild-type strain, strain 003Sm, is indicated by the broken line (relative expression equals 1). Data in both panels represent means plus standard deviations (error bars) obtained from at least three independent RNA preparations for each strain in each growth condition.

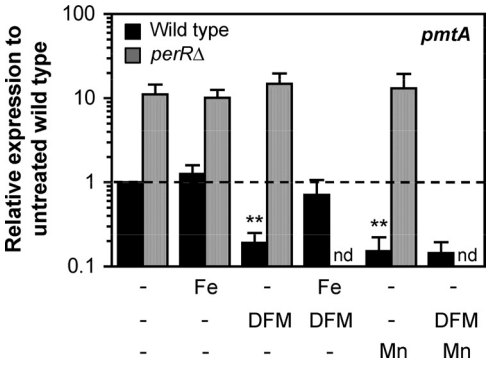

FIG. 6. Effects of iron and manganese on PerR function in the absence of peroxide. Wild-type or *perR* mutant bacteria were grown in unsupplemented broth or broth supplemented with $FeCl_3$ (Fe), $MnCl_2$ (Mn), DFM, or with equimolar concentrations of DFM and Fe or Mn. Total RNA was obtained from each strain in each growth condition, and regulation of *pmtA* was quantified by qRT-PCR. Data represent means plus standard deviations obtained from at least three independent RNA preparations for each strain in each growth condition. Wild-type expression in unsupplemented medium is indicated by the broken line (relative expression equals 1). **, $P \leq 0.005$ for comparison of *pmtA* expression in wild-type bacteria grown with added Fe versus DFM or added Mn (Student's *t* test). nd, not done.

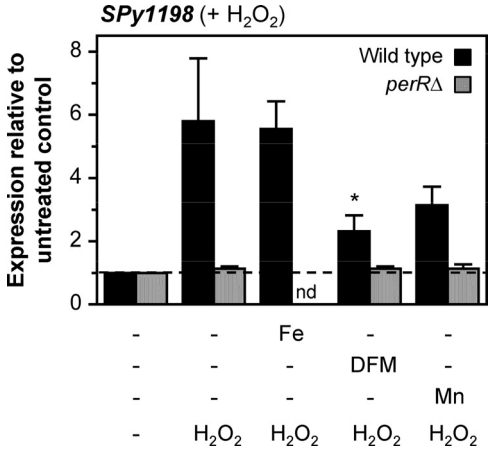

FIG. 7. Effects of metal ions on PerR function in the presence of peroxide. Wild-type or *perR* mutant bacteria were grown in unsupplemented media or media supplemented with $FeCl_3$ (Fe), $MnCl_2$ (Mn), or DFM and then challenged with 0.5 mM H_2O_2 for 15 min. Total RNA was obtained from each strain in each growth condition, and regulation of *SPy1198* was quantified by qRT-PCR. Data represent means plus standard deviations obtained from at least three independent RNA preparations for each strain in each growth condition. No change in expression in the presence of peroxide compared to expression in untreated GAS is indicated by the broken line (relative expression equals 1). *, $P < 0.05$ for comparison of *SPy1198* upregulation elicited by peroxide in unsupplemented broth versus DFM-supplemented broth (Student's *t* test). nd, not done.

PerR-regulated gene expression *in vivo* is dependent on iron and manganese. Metal dependence of PerR function was evaluated by comparing *pmtA* expression levels in bacteria grown in THY broth supplemented with iron, manganese, or the iron chelator deferoxamine mesylate (DFM) with expression levels in unsupplemented broth. Prior measurements of metal concentrations in unsupplemented THY broth indicated approximately 10 μM iron, 11 μM zinc, and 0.25 μM manganese (see Table S3 in the supplemental material). The wild-type strain or mutant strain 003Sm*perR*Δ were grown to ME phase in unsupplemented media or in media supplemented with 40 μM $FeCl_3$, 40 μM $MnCl_2$, or 40 μM DFM. Total RNA was isolated for use in qRT-PCR analyses. As shown in Fig. 6, growth of wild-type bacteria in Mn- or DFM-supplemented medium led to further repression of *pmtA* compared to expression in unsupplemented broth (~5- and ~6-fold, respectively), whereas growth in Fe-supplemented medium did not have any effect. Moreover, the *pmtA* repression effect of DFM could be reversed using an equimolar concentration of iron, but not manganese. In contrast, expression of *pmtA* in the *perR* mutant remained unchanged (>10-fold derepressed) under all conditions, a result indicating a PerR requirement for the enhanced repression detected in wild-type bacteria during growth in excess Mn or added DFM.

Further studies examined *SPy1198* upregulation in response to peroxide following growth in metal- or DFM-supplemented medium. Wild-type and *perR* mutant cultures were grown as described above and then challenged at ME phase growth with H_2O_2. For the wild type, *SPy1198* was upregulated ~6-fold in Fe-supplemented medium similar to that of the unsupplemented medium control, but this decreased substantially to 2.3-fold in the presence of DFM and to 3.1-fold in added Mn (Fig. 7). As expected, upregulation of *SPy1198* was abolished in the *perR* mutant grown in unsupplemented broth, but more interestingly, expression remained unchanged in supplemented media, a finding that also implicates PerR in the decreased upregulation levels recorded in wild-type cultures grown with added Mn or DFM. Taken together, these findings suggest iron and/or manganese binding by PerR *in vivo* and an iron requirement for maximal PerR sensitivity to peroxide.

Recombinant PerR binds iron and zinc. To verify PerR metal binding, fusions of wild-type PerR to glutathione *S*-transferase (GST-PerR) as well as of the two respective H44A and C104S mutants, GST-$PerR_{H44A}$ and GST-$PerR_{C104S}$, were expressed and purified from *E. coli* by glutathione affinity chromatography. This purification approach does not require metal-containing resin and was chosen over nickel affinity chromatography, as it has been suggested that nickel binds to recombinant PerR (26). Moreover, the possible misfolding and degradation of $PerR_{C104S}$ in *E. coli*, suggested by its degradation in GAS shown above, could potentially be prevented by its fusion to GST. All three recombinant proteins were purified at equivalent yields, and their metal content was obtained by inductively coupled plasma mass spectrometry. As shown in Table 2, these analyses revealed binding of zinc and iron to

TABLE 2. Metal content of recombinant PerR proteins

Protein	Molar ratio (metal/protein)	
	Zinc	Iron
GST-PerR	0.812	0.580
GST-PerR[a]	0.800	0.02
GST-$PerR_{H44A}$	0.829	0.567
GST-$PerR_{C104S}$	0.167	0.074
GST (control)	0.042	0.016

[a] GST-PerR purified in the presence of EDTA.

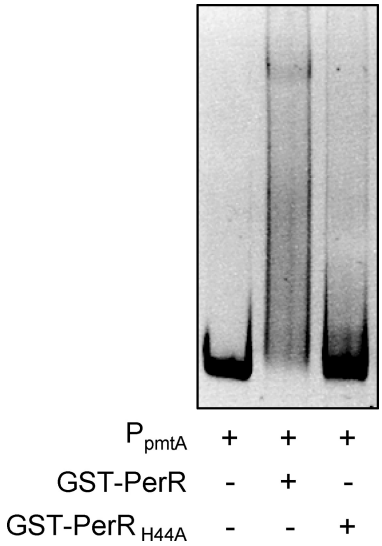

FIG. 8. Interaction of recombinant PerR with the *pmtA* promoter (P_{pmtA}). Purified wild-type GST-PerR or the H44A mutant protein GST-$PerR_{H44A}$ was mixed at a final concentration of 6 μM with 50 ng of promoter DNA and incubated at room temperature for 15 min. Following native polyacrylamide gel electrophoresis, electrophoretic mobility shift of the promoter was visualized by ethidium bromide staining.

GST-PerR at 0.81 and 0.58 atom per PerR monomer, respectively, but not to purified GST protein control. Although not fully saturated with either metal, this finding is consistent with zinc and iron binding to the predicted structural and regulatory site, respectively. In contrast, GST-$PerR_{C104S}$ showed dramatic loss of both zinc and iron (80% and 87% reduction, respectively), whereas GST-$PerR_{H44A}$ retained binding of both metals at wild-type levels. Additional purification of GST-PerR was performed in the presence of EDTA, which has been suggested to prevent iron binding and therefore prevent oxidation of histidine residues at the regulatory site that leads to loss of PerR function (38). Metal content analyses of these GST-PerR preparations yielded 0.8 zinc atom, but total loss of iron (Table 2). To assess the functions of recombinant proteins, their DNA binding capacity was evaluated in electrophoretic mobility shift assays using the *pmtA* promoter, which has been previously shown to encompass a fully conserved Per box and to bind recombinant PerR *in vitro* (21). GST-PerR purified in the absence of EDTA did not exhibit binding to *pmtA*, or any other promoter tested, possibly due to partial or full oxidation during purification. GST-PerR purified in the presence of EDTA, however, demonstrated reproducible binding and generated a high-molecular-weight DNA-protein complex, whereas GST-$PerR_{H44A}$ purified under identical conditions lacked binding capacity (Fig. 8). Interestingly, supplementation of GST-PerR with iron or manganese did not improve binding of the protein. It is proposed that although H44 is dispensable for iron binding, it is essential for PerR promoter binding and regulatory function in GAS. Moreover, C104 is required for zinc binding to the putative structural site, thereby promoting correct protein conformation and iron binding at the regulatory site.

Adaptive responses to peroxide include uncharacterized and known regulators of GAS. In addition to *SPy1198*, the peroxide stimulon encompassed PerR-independent putative regulators that have not been previously implicated in GAS defenses against ROS (see Table S2 in the supplemental material). Indeed, our finding that a major portion of the response(s) to peroxide does not require PerR suggests the existence of additional regulatory mechanism(s) coordinating GAS defenses against peroxide (and perhaps other ROS) that could encompass PerR-independent transcriptome events identified here. Two highly regulated genes in this category were (i) *SPy0146* (*sloR*) encoding a PfoR-like regulator that was 4- to 7-fold repressed at the ME phase (Table 1 and Fig. 3E) and (ii) *SPy1680* encoding a putative transcriptional activator that was ~4-fold upregulated at the LE phase (Table 1 and Fig. 3H). *SPy1680* seems to encode a typical transcriptional regulator and maps to a potential operon with four additional genes, including *npr* immediately upstream encoding a predicted NADH peroxidase. SloR exhibits high homology with orthologs in *Streptococcus* and *Clostridium.* Although previously reported to repress expression of streptolysin O in one of two GAS strains studied (59), SloR has recently been implicated in serine metabolism and/or transport, and it has been proposed that it is under direct control of the serine catabolism regulator, SerR (36).

Upregulation of the pilus biosynthesis operon discussed above prompted us also to investigate potential effects of peroxide on *msmR* (*spyM3_0103*) and *nra* (*spyM3_0097*), which encode two transcriptional regulators expressed independently from FCT-3 with opposite effects on pilus expression. MsmR activates the pilus operon and *nra* (50), whereas Nra represses the pilus operon and its own expression (34, 53). Regulation of the two genes was analyzed by qRT-PCR using RNA samples obtained from peroxide-treated and untreated wild-type strain 003Sm and primers designed on the basis of M-type 3 genome sequences. As shown in Table 1, *msmR* and *nra* were similarly upregulated in H_2O_2 by 6.6- and 4.4-fold, respectively. However, C_T values obtained in qRT-PCR analyses indicated dramatically higher *msmR* mRNA levels, suggesting higher protein levels compared to Nra (baseline C_T of ~21 for *msmR* versus ~28 for *nra*) (see Fig. S3 in the supplemental material). These data are consistent with MsmR involvement in ROS-dependent regulation of the pilus.

To further test the putative link between MsmR and pilus upregulation, the effects of peroxide were also examined in M-type 1 GAS strain 854 representing FCT-2, which encompasses the pilus synthesis operon and its transcriptional activator RofA but lacks both *msmR* and *nra* (see Fig. S4 in the supplemental material). Primers for *rofA* (*SPy0124*) and the pilus structural genes *fctA* (*SPy0128*) and *fctB* (*SPy0130*) were designed on the basis of M-type 1 strain SF370 (16), and regulation was investigated following peroxide challenge of strain 854 at ME phase growth. Unlike the strong upregulation of *msmR* and *fct* genes observed in M-type 3 strain 003Sm, a moderate (2.2-fold) upregulation of *rofA* and no change in expression of the pilus biosynthesis operon was recorded in M-type 1 GAS. In contrast, strong peroxide-mediated regulation was recorded for FCT-2-independent genes in this strain, such as a 10-fold repression of *sloR* and 15-fold activation of *SPy1198* (Fig. S4).

DISCUSSION

The data presented here support a distinct physiological role for PerR in GAS responses to peroxide. Unlike the upregulation of catalase, *ahpCF*, *mrgA*, and heme biosynthesis mediated by PerR in *B. subtilis* (25, 48), PerR in GAS mediates downregulation of DNA and protein metabolism as well as iron/heme uptake and does not upregulate any known peroxidase(s) or *mrgA*. Such a decrease in gene expression may be transient, but it would allow for DNA and protein damage repair before normal expression levels resume, similar to decreased DNA replication and cell division reported during the SOS response in other species (48, 66). The finding that a great number of repressed PerR-independent loci also encode proteins involved in DNA and protein metabolism, including rRNA/tRNA synthesis, further supports a model of decreased metabolic function upon oxidative challenge in GAS. The reduced iron/heme uptake coupled to increased Mn^{2+} import predicted by the *adc* operon upregulation in our studies is thought to lead to replacement of Fe^{2+} as a cofactor in enzymes with the Fenton-insensitive Mn^{2+}, thereby allowing optimal bacterial cell function in oxidative environments (2). Higher intracellular Mn^{2+} would also lead to increased levels of Mn^{2+}-bound PerR and therefore, a gradual decrease in responses initially driven by oxidation of Fe^{2+}-bound PerR species. Lack of downregulation of these cellular functions in a *perR* mutant would not allow time for damage repair and would result in accumulation of toxic products, which may be the reason, in part, for the attenuated capacity of *perR* mutant bacteria to resist oxidative killing by phagocytes and to colonize the pharynx (21). Moreover, the strong PerR-dependent regulation of *SPy1198* encoding a transcriptional regulator suggests that part of the PerR-mediated responses detected in our studies may be due to SPy1198 upregulation. Initial sequence examination predicts that *SPy1198* encodes both a LexA-like peptidase (C terminus) and a helix-turn-helix motif (N terminus), which is characteristic of the domain organization seen in the LexA repressor of the SOS regulon in bacteria (66). This hypothetical function of SPy1198 is in agreement with our current model of PerR involvement in regulating DNA metabolism, and its upregulation could serve to dampen the initial burst in DNA damage repair and/or restore DNA replication. Regulation of this locus seems to be a conserved response in GAS, as peroxide elicited strong upregulation in two independent isolates.

Our findings suggest that iron binding to the putative PerR regulatory site allows responses through iron oxidation but also indicate that binding of manganese and/or other metal(s) occurs in GAS *in vivo*. Manganese is known to compete with iron for a single regulatory site in *Bacillus subtilis* PerR ($PerR_{Bsu}$); however, the possibility that it binds to an independent GAS PerR ($PerR_{GAS}$) site to modulate its function cannot be ruled out. The regulatory site requires H44 and possibly one or more of the three other conserved residues, D93, H99, and D112. Loss of regulation in $PerR_{H44A}$-expressing GAS and conservation of residues in the predicted regulatory site suggest that the latter is essential to $PerR_{GAS}$ function. Moreover, the conserved structural site requires C104 for stability and coordination of zinc binding, as indicated by the rapid degradation of $PerR_{C104S}$ *in vivo* and the dramatic reduction in zinc (and iron) content of the recombinant mutant protein. Our result that GST-$PerR_{H44A}$ lacks promoter binding even though it contains wild-type iron levels suggests that H44 is essential for wild-type protein conformation and regulatory function. This mutant seems to be different from $PerR_{H37A}$ in *Bacillus*, which exhibits an iron binding affinity severalfold lower than that of the wild-type protein (64). Promoter binding of EDTA-treated GST-PerR is consistent with the hypothesis that iron is not required for binding *per se*, but seems to be required for optimal PerR-regulated responses to peroxide and would serve to mediate PerR oxidation levels and function. Recent evidence indicates that three additional residues (Y92, E114, and H128) coordinate iron binding and stabilize an active $PerR_{Bsu}$ conformation (43); however, these residues are not conserved in $PerR_{GAS}$. Moreover, the apparent limited overlap between the genes controlled by $PerR_{GAS}$ in peroxide with those identified by comparison of wild-type and *perR* mutant transcriptomes in the absence of stress (see Table S2 in the supplemental material) further indicates an overall unique molecular function mechanism of PerR in *Streptococcus*. Oxidation of $PerR_{GAS}$ may not lead to its release from bound promoters, a model that would explain the lack of peroxide-mediated derepression of *pmtA* and other PerR-dependent genes identified previously in the absence of peroxide. Histidine- or GST-tagged recombinant PerR obtained in current or previous studies (21) did not bind to promoters of PerR-dependent loci identified here (*adcRCB*, *SPy1198*, and *SPy2111-nrdD*) although scanning of promoter sequences revealed Per box-like motifs upstream of *SPy1198* and *SPy2111* (I. Gryllos, unpublished data). It remains possible that regulation of these genes is not direct or that $PerR_{GAS}$ requires other factors and/or conditions for binding to certain promoters.

In addition to newly characterized PerR-regulated gene expression, identification of PerR-independent upregulated responses in peroxide provides further insight into GAS defense strategies against oxidative stress. The stronger activation of DNA damage repair mechanisms over ROS neutralizing enzymes observed in the current study implies a key role of the former in GAS survival under oxidative conditions. DNA repair is considered the primary defense mechanism against ROS in certain bacterial species including *Staphylococcus* (9, 11). Moreover, strong upregulation of cofactor metabolism and *lplA* (*SPy1214*) indicates a contribution of lipoic acid protein modification in streptococcal resistance to oxidative damage. GAS carries a gene that encodes a second LplA homologue (*SPy1033*) (61) that is not upregulated by peroxide, a finding that implicates SPy1214 in independent or overlapping lipoylation reactions required for optimal survival in oxidative environments. Reduced lipoic acids (dihydrolipoic acids) on pyruvate dehydrogenase complexes have been shown to contribute to mycobacterial defenses against oxidative stress by providing the reducing capacity to AhpC for detoxification of peroxides and peroxynitrites (8, 63). Additionally, lipoic acids can directly (i) detoxify ROS, (ii) chelate iron, which generates ROS via the Fenton reaction, and (iii) reduce thioredoxins as well as GSSG to GSH (45). Induction of the *suf* locus is likely to be essential for Fe-S maintenance and therefore optimal GAS resistance to oxidative damage. In *E. coli*, OxyR-mediated activation of the Suf system by peroxide is critical for both *de novo* synthesis and repair of oxidized Fe-S, even though this

species carries a gene that encodes a protein involved in a second Fe-S biosynthesis mechanism (29).

Furthermore, the strong PerR-independent regulation of putative or known regulatory loci recorded in our studies is thought to be of significance, as each of these could control expression of one or more products modulating GAS defenses against ROS. Peroxide-mediated activation of MsmR and the pilus biosynthesis operon is expected to enhance GAS virulence. Pili have been associated with adherence to human tonsil epithelium and to primary human epithelial cells *in vitro* (1, 44); thus, increased expression elicited by ROS during throat colonization would augment GAS adherence to the pharyngeal mucosa and promote establishment of infection. Upregulation of MsmR could have extra implications on colonization, as it is known to activate expression of fibronectin-binding proteins and other adhesins, in addition to the pilus (50). Increased FCT locus expression in M-type 3, but not M-type 1, GAS predicts strain-dependent effects of peroxide on pilus and other MsmR-regulated loci.

In summary, identification of global transcriptional changes elicited by peroxide reveals uncharacterized streptococcal defense mechanisms and a unique physiological role of PerR in bacterial responses to oxidative stress. The differential regulatory capacity of PerR influenced by environmental metal concentrations and ROS predicts a dynamic pattern of regulation *in vivo* that is likely to be adaptive to the host environment and the innate immune responses encountered. Future examination of newly identified PerR-dependent and -independent defense mechanisms will expand our knowledge of streptococcal virulence strategies and pathogenesis in the human host.

ACKNOWLEDGMENTS

This work was supported in part by NIH grant AI080802 to I.G.

We thank Charles Langmuir and Zhongxing Chen at the Department of Earth and Planetary Sciences, Harvard University, for help with mass spectrometry analyses and Alessandro Muzzi for help with bioinformatics. We also thank John Helmann and Gregory Smaldone for helpful discussions.

REFERENCES

1. **Abbot, E. L., et al.** 2007. Pili mediate specific adhesion of *Streptococcus pyogenes* to human tonsil and skin. Cell. Microbiol. **9:**1822–1833.
2. **Anjem, A., S. Varghese, and J. A. Imlay.** 2009. Manganese import is a key element of the OxyR response to hydrogen peroxide in *Escherichia coli*. Mol. Microbiol. **72:**844–858.
3. **Bates, C. S., G. E. Montanez, C. R. Woods, R. M. Vincent, and Z. Eichenbaum.** 2003. Identification and characterization of a *Streptococcus pyogenes* operon involved in binding of hemoproteins and acquisition of iron. Infect. Immun. **71:**1042–1055.
4. **Beres, S. B., et al.** 2002. Genome sequence of a serotype M3 strain of group A *Streptococcus*: phage-encoded toxins, the high-virulence phenotype, and clone emergence. Proc. Natl. Acad. Sci. U. S. A. **99:**10078–10083.
5. **Brenot, A., K. Y. King, and M. G. Caparon.** 2005. The PerR regulon in peroxide resistance and virulence of *Streptococcus pyogenes*. Mol. Microbiol. **55:**221–234.
6. **Brenot, A., K. Y. King, B. Janowiak, O. Griffith, and M. G. Caparon.** 2004. Contribution of glutathione peroxidase to the virulence of *Streptococcus pyogenes*. Infect. Immun. **72:**408–413.
7. **Brenot, A., B. F. Weston, and M. G. Caparon.** 2007. A PerR-regulated metal transporter (PmtA) is an interface between oxidative stress and metal homeostasis in *Streptococcus pyogenes*. Mol. Microbiol. **63:**1185–1196.
8. **Bryk, R., C. D. Lima, H. Erdjument-Bromage, P. Tempst, and C. Nathan.** 2002. Metabolic enzymes of mycobacteria linked to antioxidant defense by a thioredoxin-like protein. Science **295:**1073–1077.
9. **Buchmeier, N. A., et al.** 1995. DNA repair is more important than catalase for *Salmonella* virulence in mice. J. Clin. Invest. **95:**1047–1053.
10. **Carapetis, J. R., A. C. Steer, E. K. Mulholland, and M. Weber.** 2005. The global burden of group A streptococcal diseases. Lancet Infect. Dis. **5:**685–694.
11. **Chang, W., D. A. Small, F. Toghrol, and W. E. Bentley.** 2006. Global transcriptome analysis of *Staphylococcus aureus* response to hydrogen peroxide. J. Bacteriol. **188:**1648–1659.
12. **Chen, L., L. Keramati, and J. D. Helmann.** 1995. Coordinate regulation of *Bacillus subtilis* peroxide stress genes by hydrogen peroxide and metal ions. Proc. Natl. Acad. Sci. U. S. A. **92:**8190–8194.
13. **Cox, M. M.** 2007. Regulation of bacterial RecA protein function. Crit. Rev. Biochem. Mol. Biol. **42:**41–63.
14. **Dintilhac, A., G. Alloing, C. Granadel, and J. P. Claverys.** 1997. Competence and virulence of *Streptococcus pneumoniae*: Adc and PsaA mutants exhibit a requirement for Zn and Mn resulting from inactivation of putative ABC metal permeases. Mol. Microbiol. **25:**727–739.
15. **Falugi, F., et al.** 2008. Sequence variation in group A *Streptococcus* pili and association of pilus backbone types with Lancefield T serotypes. J. Infect. Dis. **198:**1834–1841.
16. **Ferretti, J. J., et al.** 2001. Complete genome sequence of an M1 strain of *Streptococcus pyogenes*. Proc. Natl. Acad. Sci. U. S. A. **98:**4658–4663.
17. **Gerlach, D., W. Reichardt, and S. Vettermann.** 1998. Extracellular superoxide dismutase from *Streptococcus pyogenes* type 12 strain is manganese-dependent. FEMS Microbiol. Lett. **160:**217–224.
18. **Gibson, C. M., and M. G. Caparon.** 1996. Insertional inactivation of *Streptococcus pyogenes sod* suggests that *prtF* is regulated in response to a superoxide signal. J. Bacteriol. **178:**4688–4695.
19. **Gon, S., and J. Beckwith.** 2006. Ribonucleotide reductases: influence of environment on synthesis and activity. Antioxid. Redox Signal. **8:**773–780.
20. **Green, D. E., T. W. Morris, J. Green, J. E. Cronan, Jr., and J. R. Guest.** 1995. Purification and properties of the lipoate protein ligase of *Escherichia coli*. Biochem. J. **309:**853–862.
21. **Gryllos, I., et al.** 2008. PerR confers phagocytic killing resistance and allows pharyngeal colonization by group A *Streptococcus*. PLoS Pathog. **4:**e1000145.
22. **Gryllos, I., et al.** 2007. Mg^{2+} signalling defines the group A streptococcal CsrRS (CovRS) regulon. Mol. Microbiol. **65:**671–683.
23. **Gryllos, I., et al.** 2008. Induction of group A *Streptococcus* virulence by a human antimicrobial peptide. Proc. Natl. Acad. Sci. U. S. A. **105:**16755–16760.
24. **Hanks, T. S., M. Liu, M. J. McClure, and B. Lei.** 2005. ABC transporter FtsABCD of *Streptococcus pyogenes* mediates uptake of ferric ferrichrome. BMC Microbiol. **5:**62.
25. **Helmann, J. D., et al.** 2003. The global transcriptional response of *Bacillus subtilis* to peroxide stress is coordinated by three transcription factors. J. Bacteriol. **185:**243–253.
26. **Herbig, A. F., and J. D. Helmann.** 2001. Roles of metal ions and hydrogen peroxide in modulating the interaction of the *Bacillus subtilis* PerR peroxide regulon repressor with operator DNA. Mol. Microbiol. **41:**849–859.
27. **Horsburgh, M. J., M. O. Clements, H. Crossley, E. Ingham, and S. J. Foster.** 2001. PerR controls oxidative stress resistance and iron storage proteins and is required for virulence in *Staphylococcus aureus*. Infect. Immun. **69:**3744–3754.
28. **Ibarra, J. R., et al.** 2008. Role of the Nfo and ExoA apurinic/apyrimidinic endonucleases in repair of DNA damage during outgrowth of *Bacillus subtilis* spores. J. Bacteriol. **190:**2031–2038.
29. **Jang, S., and J. A. Imlay.** 2010. Hydrogen peroxide inactivates the *Escherichia coli* Isc iron-sulphur assembly system, and OxyR induces the Suf system to compensate. Mol. Microbiol. **78:**1448–1467.
30. **Janulczyk, R., J. Pallon, and L. Bjorck.** 1999. Identification and characterization of a *Streptococcus pyogenes* ABC transporter with multiple specificity for metal cations. Mol. Microbiol. **34:**596–606.
31. **Kanehisa, M., and S. Goto.** 2000. KEGG: Kyoto Encyclopedia of Genes and Genomes. Nucleic Acids Res. **28:**27–30.
32. **Kessler, D.** 2006. Enzymatic activation of sulfur for incorporation into biomolecules in prokaryotes. FEMS Microbiol. Rev. **30:**825–840.
33. **King, K. Y., J. A. Horenstein, and M. G. Caparon.** 2000. Aerotolerance and peroxide resistance in peroxidase and PerR mutants of *Streptococcus pyogenes*. J. Bacteriol. **182:**5290–5299.
34. **Kreikemeyer, B., et al.** 2007. The *Streptococcus pyogenes* serotype M49 Nra-Ralp3 transcriptional regulatory network and its control of virulence factor expression from the novel *eno ralp3 epf sagA* pathogenicity region. Infect. Immun. **75:**5698–5710.
35. **Larkin, M. A., et al.** 2007. Clustal W and Clustal X version 2.0. Bioinformatics **23:**2947–2948.
36. **LaSarre, B., and M. J. Federle.** 2011. Regulation and consequence of serine catabolism in *Streptococcus pyogenes*. J. Bacteriol. **193:**2002–2012.
37. **Lee, J. W., and J. D. Helmann.** 2006. Biochemical characterization of the structural Zn^{2+} site in the *Bacillus subtilis* peroxide sensor PerR. J. Biol. Chem. **281:**23567–23578.
38. **Lee, J. W., and J. D. Helmann.** 2006. The PerR transcription factor senses H_2O_2 by metal-catalysed histidine oxidation. Nature **440:**363–367.
39. **Lei, B., et al.** 2003. Identification and characterization of HtsA, a second heme-binding protein made by *Streptococcus pyogenes*. Infect. Immun. **71:**5962–5969.
40. **Lei, B., et al.** 2002. Identification and characterization of a novel heme-

associated cell surface protein made by *Streptococcus pyogenes*. Infect. Immun. **70:**4494–4500.
41. **Loo, C. Y., K. Mitrakul, I. B. Voss, C. V. Hughes, and N. Ganeshkumar.** 2003. Involvement of the *adc* operon and manganese homeostasis in *Streptococcus gordonii* biofilm formation. J. Bacteriol. **185:**2887–2900.
42. **Lu, A. L., X. Li, Y. Gu, P. M. Wright, and D. Y. Chang.** 2001. Repair of oxidative DNA damage: mechanisms and functions. Cell Biochem. Biophys. **35:**141–170.
43. **Ma, Z., J. W. Lee, and J. D. Helmann.** 2011. Identification of altered function alleles that affect *Bacillus subtilis* PerR metal ion selectivity. Nucleic Acids Res. **39:**5036–5044.
44. **Manetti, A. G., et al.** 2007. *Streptococcus pyogenes* pili promote pharyngeal cell adhesion and biofilm formation. Mol. Microbiol. **64:**968–983.
45. **Moini, H., L. Packer, and N. E. Saris.** 2002. Antioxidant and prooxidant activities of alpha-lipoic acid and dihydrolipoic acid. Toxicol. Appl. Pharmacol. **182:**84–90.
46. **Mora, M., et al.** 2005. Group A *Streptococcus* produce pilus-like structures containing protective antigens and Lancefield T antigens. Proc. Natl. Acad. Sci. U. S. A. **102:**15641–15646.
47. **Morris, T. W., K. E. Reed, and J. E. Cronan, Jr.** 1994. Identification of the gene encoding lipoate-protein ligase A of *Escherichia coli*. Molecular cloning and characterization of the *lplA* gene and gene product. J. Biol. Chem. **269:**16091–16100.
48. **Mostertz, J., C. Scharf, M. Hecker, and G. Homuth.** 2004. Transcriptome and proteome analysis of *Bacillus subtilis* gene expression in response to superoxide and peroxide stress. Microbiology **150:**497–512.
49. **Nakata, M., et al.** 2009. Mode of expression and functional characterization of FCT-3 pilus region-encoded proteins in *Streptococcus pyogenes* serotype M49. Infect. Immun. **77:**32–44.
50. **Nakata, M., A. Podbielski, and B. Kreikemeyer.** 2005. MsmR, a specific positive regulator of the *Streptococcus pyogenes* FCT pathogenicity region and cytolysin-mediated translocation system genes. Mol. Microbiol. **57:**786–803.
51. **O'Loughlin, R. E., et al.** 2007. The epidemiology of invasive group A streptococcal infection and potential vaccine implications: United States, 2000-2004. Clin. Infect. Dis. **45:**853–862.
52. **Podbielski, A., et al.** 1996. Molecular characterization of group A streptococcal (GAS) oligopeptide permease (*opp*) and its effect on cysteine protease production. Mol. Microbiol. **21:**1087–1099.
53. **Podbielski, A., M. Woischnik, B. A. Leonard, and K. H. Schmidt.** 1999. Characterization of nra, a global negative regulator gene in group A streptococci. Mol. Microbiol. **31:**1051–1064.
54. **Poyart, C., et al.** 2001. Contribution of Mn-cofactored superoxide dismutase (SodA) to the virulence of *Streptococcus agalactiae*. Infect. Immun. **69:**5098–5106.
55. **Riboldi, G. P., H. Verli, and J. Frazzon.** 2009. Structural studies of the *Enterococcus faecalis* SufU [Fe-S] cluster protein. BMC Biochem. **10:**3.
56. **Ricci, S., R. Janulczyk, and L. Bjorck.** 2002. The regulator PerR is involved in oxidative stress response and iron homeostasis and is necessary for full virulence of *Streptococcus pyogenes*. Infect. Immun. **70:**4968–4976.
57. **Romantsov, T., Z. Guan, and J. M. Wood.** 2009. Cardiolipin and the osmotic stress responses of bacteria. Biochim. Biophys. Acta **1788:**2092–2100.
58. **Rosch, J. W., F. F. Hsu, and M. G. Caparon.** 2007. Anionic lipids enriched at the ExPortal of *Streptococcus pyogenes*. J. Bacteriol. **189:**801–806.
59. **Savic, D. J., W. M. McShan, and J. J. Ferretti.** 2002. Autonomous expression of the *slo* gene of the bicistronic *nga-slo* operon of *Streptococcus pyogenes*. Infect. Immun. **70:**2730–2733.
60. **Smoot, J. C., et al.** 2002. Genome sequence and comparative microarray analysis of serotype M18 group A *Streptococcus* strains associated with acute rheumatic fever outbreaks. Proc. Natl. Acad. Sci. U. S. A. **99:**4668–4673.
61. **Spalding, M. D., and S. T. Prigge.** 2010. Lipoic acid metabolism in microbial pathogens. Microbiol. Mol. Biol. Rev. **74:**200–228.
62. **Sun, X., R. Ge, J. F. Chiu, H. Sun, and Q. Y. He.** 2008. Lipoprotein MtsA of MtsABC in *Streptococcus pyogenes* primarily binds ferrous ion with bicarbonate as a synergistic anion. FEBS Lett. **582:**1351–1354.
63. **Tian, J., et al.** 2005. *Mycobacterium tuberculosis* appears to lack alpha-ketoglutarate dehydrogenase and encodes pyruvate dehydrogenase in widely separated genes. Mol. Microbiol. **57:**859–868.
64. **Traore, D. A., et al.** 2009. Structural and functional characterization of 2-oxo-histidine in oxidized PerR protein. Nat. Chem. Biol. **5:**53–59.
65. **Tsou, C. C., et al.** 2008. An iron-binding protein, Dpr, decreases hydrogen peroxide stress and protects *Streptococcus pyogenes* against multiple stresses. Infect. Immun. **76:**4038–4045.
66. **Walker, G. C.** 1985. Inducible DNA repair systems. Annu. Rev. Biochem. **54:**425–457.
67. **Yellaboina, S., J. Seshadri, M. S. Kumar, and A. Ranjan.** 2004. PredictRegulon: a web server for the prediction of the regulatory protein binding sites and operons in prokaryote genomes. Nucleic Acids Res. **32:**W318–W320.